J Mol Model (2016) 22: 187
DOI 10.1007/s00894-016-3034-9

ORIGINAL PAPER

Z-Isomers of (4α→6″, 2α→*O*→1″)-phenylflavan substituted with R′=R=OH. Conformational properties, electronic structure and aqueous solvent effects

Erika N. Bentz[1] · **Alicia B. Pomilio**[2] · **Rosana M. Lobayan**[1]

Received: 24 September 2015 / Accepted: 9 June 2016 / Published online: 22 July 2016

Abstract Procyanidins are highly hydroxylated polymers known as antioxidant compounds, thereby exhibiting beneficial effects. These compounds are protective agents against oxidative stress and the damage induced by free radicals in membranes and nucleic acids. This paper describes a study of the conformational space of (4α→6″, 2α→*O*→1″)-phenylflavan substituted with R′=R=OH as part of a larger study of similar structures with different substitutions. The relationships between aqueous solution–vacuum variations of some properties were studied, as well as the stabilization and reactivity of (4α→6″, 2α→*O*→1″)-phenylflavan substituted with R′=R=H, R′=H, R=OH, R′=R=OH, and (+)-catechin. The variations in geometric parameters and electronic properties due to conformational changes, as well as the effects of substituents and polar solvents, were evaluated and analyzed. Bader's theory of atoms in molecules was applied to characterize intramolecular interactions, along with a natural bond orbital analysis for each conformer described. The molecular electrostatic potential was rationalized by charge delocalization mechanisms and interatomic intramolecular interactions, relating them to the structural changes and topological properties of the electron charge density. Molecular polarizability and permanent electric dipole moment values were estimated. The results show the importance of a knowledge of the conformational space, and values for each conformer. Based on our previous results, we showed the existence of electron charge delocalization mechanisms acting cooperatively as "delocalization routes", showing interactions between different rings not even sharing the same plane. These "delocalization routes" were more effective for (4α→6″, 2α→*O*→1″)-phenylflavan substituted with R′=R=OH than for (+)-catechin, and are proposed as adding insight into the structure–antioxidant activity relationship of flavans.

Keywords (4α→6″, 2α→O→1″)- phenylflavans · Antioxidants · Density functional theory · Aqueous solvent effect · PCM model · Atoms in molecules · Natural bond orbital analysis · Molecular polarizability

Introduction

Polyphenolics are a large group of secondary metabolites that have structures with aromatic rings substituted with at least one OH, other oxygenated groups, and conjugated double bonds that are together responsible for their antioxidant activities. Extractable polyphenolics can be classified according to their chemical structure as simple phenolic acids, and flavonoids, which in turn are subdivided into flavones, flavonols, flavanols or catechins, flavanones, anthocyanins, aurones, chalcones, isoflavones, biflavonoids, condensed tannins, and other compounds.

Condensed tannins, or proanthocyanidins, are polymeric structures formed by the condensation of flavan-3-ols. These proanthocyanidins can be procyanidins, with a 3,4-dihydroxy pattern in ring B (comprising only epicatechin moieties);

Electronic supplementary material The online version of this article (doi:10.1007/s00894-016-3034-9) contains supplementary material, which is available to authorized users.

✉ Rosana M. Lobayan
rmlb@exa.unne.edu.ar

[1] Departamento de Física, Facultad de Ciencias Exactas y Naturales y Agrimensura, Universidad Nacional del Nordeste, Avda. Libertad 5300, 3400 Corrientes, Argentina

[2] Instituto de Bioquímica y Medicina Molecular [IBIMOL (ex PRALIB), UBA-CONICET], Facultad de Farmacia y Bioquímica, Universidad de Buenos Aires, Junín 956, C1113AAD Buenos Aires, Argentina

prodelphinidins, with a 3,4,5-trihydroxy pattern in ring B; and propelargonidins, with a 4-hydroxyl in ring B—the latter being less common in foods.

Proanthocyanidins are consumed widely in fruits and vegetables, and also in some drinks, such as red wine, green tea, and chocolate. The type and amount of these compounds in plants vary widely [1]. The exact composition of proanthocyanidins in foods remains controversial due to the numerous structures, degree of polymerization, and different quantitative analytical techniques used [1–3].

Most research has focused on proanthocyanidins, highly hydroxylated polymers, due to their antioxidant properties [4, 5], thereby showing many beneficial effects [6, 7]. These compounds are protective agents against oxidative stress and the damage induced by free radicals in membranes and nucleic acids [8].

In this work, the conformational space of (4α→6″, 2α→*O*→1″)-phenylflavan substituted with R′=R=OH was studied, as part of a larger study of similar structures with different substitutions [9–12]. Also, variations in geometric parameters and electronic properties due to conformational changes, as well as the effects of substituents and polar solvents, were analyzed.

Bader's theory of atoms in molecules (AIM) and natural bond orbital (NBO) analysis were used to characterize intramolecular interactions for each conformer described. Molecular electrostatic potentials (MEPs) were also analyzed on the basis of the AIM and NBO results. Molecular polarizability and permanent electric dipole moment values were estimated.

Based on our previous results [9–12], the present study focused on further analysis of the effect of aqueous solvents, thereby establishing the relationships between solution–vacuum variations of some properties, as well as the stabilization and reactivity of these compounds in a polar solvent.

Methods

The study of the conformational space in gas phase of (4α→6″, 2α→*O*→1″)-phenylflavan substituted with OH groups in rings B and D was performed using molecular dynamics (MD) calculations [13] to obtain starting conformations. Four structures were selected, namely 1, 2, 3 and 4, corresponding to dihedral angles (τ), C3—C2—C1′—C2′ of ≈90°, ≈270°, ≈180° and ≈0°, respectively. These structures arose from the rotation of ring B around the C2—C1′ bond, and were further analyzed by a rigid scan setting the dihedral angle (τ), C3—C2—C1′—C2′ in steps, thus obtaining the profiles of the potential energy surfaces. The effects of free rotation around the C—O bonds of HO-3″ and HO-5″ (resorcinol-type ring, "D"), and HO-3′ and HO-4′ (catechol-type ring, "B"), and rotation around the C2—C1′ bond (Fig. 1) were taken into account by rigid scans. The structures of type 1 and 2 (3 and 4) were called Z_1 (Z_2). Taking into account the lowest energy conformations, and the corresponding transition states, reoptimizations were carried out with fully relaxed geometries by density functional theory (DFT) with B3LYP hybrid functional [14, 15], and 6-31G(d,p) basis set, as implemented in Gaussian 03 [16]. Harmonic vibrational frequencies were calculated at the same level to support the occurrence of true minimum energy structures, and transition states as well as to evaluate zero point energy (ZPE) corrections. Energy values were refined by single point-type calculations at the 6-311++ G (d,p) basis set, next corrected by ZPE at the B3LYP/6-31G(d,p) level.

The lowest energy conformers in the gas phase were reoptimized, considering the effect of solvent, by the polarizable continuum model (PCM) [17] at the same level of theory. The polarizable dielectric medium was described by the dielectric constant (ε = 78.39 for water). The values of surface area, and cavity volume were in the ranges of 402.80–405.63 Å^2 and 454.6–457.69 Å^3, respectively. At the same calculation level, ZPEs were obtained to correct all energy terms.

MEPs were calculated using Gaussian 03 software, and displayed by Molekel 4.0 software [18]. MEP contours were drawn with Multiwfn 3.3.2. software [19].

Topological analysis was performed with the PROAIM software [20] at the B3LYP level, and 6-311++G (d,p) basis set. The most significant local topological properties in bond critical points (BCPs) of the chemical bonds were characterized both in gas phase and in a simulated aqueous solvent.

NBO analysis [21] was carried out at the same level as AIM calculations, and allowed electron charge delocalizations typical of the structures under study to be described. Hyperconjugative interactions that defined the stability order for all conformers, and charge delocalization trends were characterized. For each NBO donor (*i*), and each NBO acceptor (*j*), the second-order perturbation energy ($E^{(2)}$) associated with *i*/*j* delocalization was as follows:

$$E^{(2)} = -n_i \frac{F_{ij}^2}{\varepsilon_j - \varepsilon_i}$$

where n_i is the occupation or population of the donor orbital *i*; ε_i and ε_j are the orbital energies involved in the interaction, and $F_{(i,j)}$ is the element *i*,*j* of the Fock matrix.

Variation of parameters of interest (*x*) derived from topological, NBO and MEP analyses in aqueous solution was quantified by calculating percentage differences relative to values under vacuum:

$$\%\Delta x = \frac{x(solution) - x(vacuum)}{x(vacuum)}$$

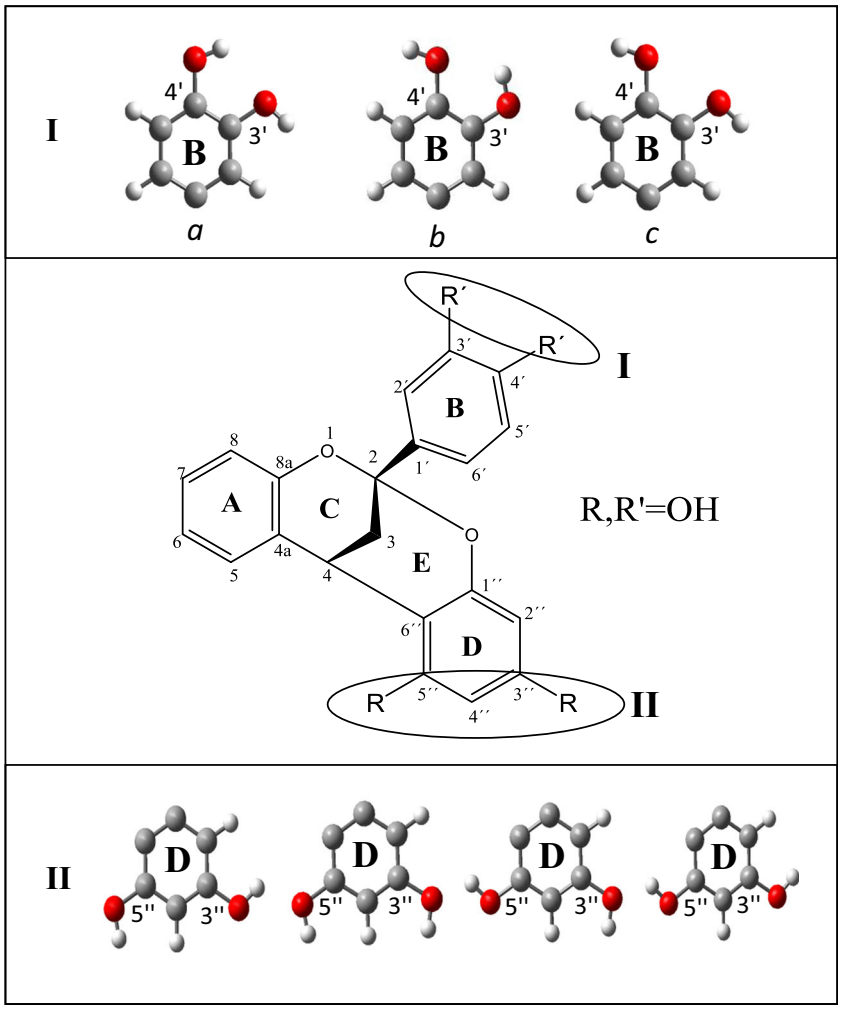

Fig. 1 Structure of (4α→6″, 2α→*O*→1″)-phenylflavan substituted with R′=R=OH. Numbering used for analysis is indicated

Molecular polarizability <α>, and permanent electric dipole moment μ were also studied. The <α> values were calculated as:

$$\langle \alpha \rangle = \frac{1}{3}\left(\alpha_{xx} + \alpha_{yy} + \alpha_{zz}\right)$$

where tensor components (α) were obtained from the second derivative of the energy relative to Cartesian components of applied electric field (ε), $\alpha = [\partial^2 E/\partial \varepsilon^2]$. The weight of different conformers was considered for <α> values; the statistical average value was calculated from the Maxwell-Boltzmann distribution of polarizability at 298.15 K,

$$< \alpha >= \sum_i < \alpha_i > \exp\left(\frac{-E_i}{RT}\right) \Big/ \sum_i \exp\left(\frac{-E_i}{RT}\right)$$

The entire conformational space was also considered for μ values, and, therefore, a similar statistical average was calculated on each Cartesian component,

$$\left\langle \mu_j \right\rangle = \sum_i \mu_{j,i} \exp\left(-\frac{E_i}{RT}\right) \Big/ \sum_i \exp\left(-\frac{E_i}{RT}\right)$$

with $j = x, y, z$; where E_i was the relative energy of conformer i, and $\mu_{j.i}$ was component j of conformer i. Then, the statistical average of the total permanent electric dipole moment magnitude was obtained by the Maxwell-Boltzmann distribution.

$$\langle \mu \rangle = \sqrt{\langle \mu_x \rangle^2 + \left\langle \mu_y \right\rangle^2 + \langle \mu_z \rangle^2}$$

Results and discussion

Conformational analysis

A study of the conformers throughout the conformational space was carried out; conformers obtained by changing the O–H arrangements of ring D are indicated by C and T subscripts, referring to syn (cis) and anti (trans) configurations of

H—O3″ and H—O5″ bonds of the resorcinol ring (ring D) relative to the C3″—C4″ and C5″—C4″ bonds, respectively (line II, Fig. 1). The mean values of H—O3″—C3″—C4″ and H—O5″—C5″—C4″ dihedral angles were close to 180.0° (anti), and 0.0° (syn). In turn, the O–H arrangements of the catechol ring (ring B) allowed the conformers to be classified into three groups, namely *a*, *b*, and *c*. Therefore, structure a_{CT} was that in which the hydroxyl H atom that would form an intramolecular hydrogen bond (HB) was attached to C-4′; b_{CT}, in which the hydroxyl H atom that would form an intramolecular HB was attached to C-3′, and, finally, c_{CT} accounted for an OH arrangement that would not form any intramolecular HB in ring B (line I, Fig. 1). Consequently, groups were characterized by the hydroxyl H atom involved in the HB.

In total, 48 conformers were obtained, confirming minima energy structures on the hypersurface of the molecules by vibrational analysis.

On the basis of energy stability, and relative Maxwell-Boltzmann population at room temperature (298.15 K), a subset of 12 CT-type conformers (Table 1) with a relative population of 74.54 % was selected. The relative population of CT conformers was one order of magnitude higher than that of CC conformers, while that of CC conformers was one order of magnitude higher than those of TC and TT conformers. Moreover, the energy gap between *a* and *b* structures with respect to *c*-type led to a tiny population of the latter (Table 1), which thus were not considered further in this next study.

By a rigid scan at the B3LYP/6-31G(d,p) level rotating ring B [setting dihedral angle (τ), C3—C2—C1′—C2′] around the C2—C1′ bond in 30.0° steps for a_{CT}, b_{CT}, and c_{CT} structures (Figs. S1, S2 and S3; Supplementary Material), the profiles of potential energy surfaces were obtained, showing two minima, Z_1 and Z_2. The low barrier value (less than 3.0 kcal mol^{-1}) suggested the coexistence of both Z_1 and Z_2 conformers at room temperature, as previously reported for similar compounds [9–12]. The C3—C2—C1′—C2′ dihedral angle indicated that ring B position relative to ring C was 88.0° as mean value for all Z_1 structures (Fig. 2; $a1_{CT}$ and $a2_{CT}$ conformers), and close to 0.0° for Z_2 (Fig. 2; $a3_{CT}$ and $a4_{CT}$ conformers).

The Z_1 conformers were the most stable for each group, having a higher relative population with τ close to 270.0° for the minima of a_{CT} and b_{CT}, as shown in Table 1. Therefore, in gas phase, the stability order was, $a2_{CT} > a1_{CT} > b2_{CT} > b1_{CT}$. The most stable structure was $a2_{CT}$ with an energy value of −791,230.15 kcal mol^{-1}. The energy differences of the other conformers with respect to the most stable one were, on average, 0.17 kcal mol^{-1} for type *a* structures; 0.40 kcal mol^{-1} for *b*; and 4.20 kcal mol^{-1} for *c*. The energy differences of Z_2 conformers with respect to the most stable structure were, on average, 2.02 kcal mol^{-1} for type *a* structures; 2.24 kcal mol^{-1} for *b*; and 6.15 kcal mol^{-1} for *c*.

The energy values of Z_1 conformers were, on average, 1.96 kcal mol^{-1} less than those of Z_2. The energy gap between Z_1 and Z_2 conformers calculated by Maxwell-Boltzmann distribution at 298.15 K led to relative populations of 60.46 %, 34.39 %, and 0.05 % for Z_1 conformers of types *a*, *b*, and *c*, respectively, while the sums of the relative Z_2 populations accounted for 2.87 %, 1.53 %, and 0.00 % for *a*, *b*, and *c* type structures, respectively (Table 1). The relative weight of Z_2 structures showed that these structures might be taken into account; although slightly lower than those of similar compounds [9–12], their relative weight was up to two orders of magnitude higher than that of (+)-catechin [12].

The electronic energies of the transition states in gas phase at the B3LYP/6-31G(d,p) level of theory are shown in Table S1 (Supplementary Material).

Full (τ) angle rotation in ± 30° steps in both species (a_{CT} and b_{CT}) led to two transition states (TS), TS2 and TS3, for Z_2 rotamer, and two TS (TS1 and TS4) for Z_1.

Effects of aqueous solvent on conformational analysis

The same type of structures were obtained in vacuum as in PCM-simulated aqueous solution for phenylflavan substituted with R′=R=OH throughout the conformational space, indicated as xy_z with x = a,b,c; y = 1,2,3,4; and z = CT, CC, TC, TT. Then, two Z_1 conformers (y = 1, 2), and two Z_2 (y = 3, 4) were obtained for each "xz" subgroup (Figure S4; Supplementary Material). The inclusion of the solvent introduced small changes in the relative energy order. Therefore, the stability order was, $a2_{CT} > b1_{CT} > a1_{CT} > b2_{CT}$. The values of the electronic energies, and the relative populations in aqueous phase are shown in Table 1.

Energies relative to the most stable conformer were decreased in solution, as reported for similar compounds [11, 12] as well as pelargonidin and other anthocyanidins in PCM-simulated aqueous solution at the B3LYP/6-31++G(d,p) level of theory [22]. Energy differences between structures in gas phase and in aqueous solution averaged 13.10 kcal mol^{-1}. All conformers were stabilized in solution, but Z_2 rotamers were more stabilized than Z_1. The relative population of Z_2 rotamers increased from 4.5 % in gas phase to 7.4 % in aqueous solution. In turn, (+)-catechin showed a weight of only 0.17 % for Z_2 in vacuum, and was absent in aqueous solution [12].

The effect of solvent on structure stabilization was not uniform for all conformers. Relative populations at 298.15 K calculated by Maxwell-Boltzmann distribution showed considerable variation in solution, especially for the most stable conformers. In gas phase, the sum of the relative populations was 63.41 % for a_{CT}, 36.52 % for b_{CT}, and 0.06 % for c_{CT}. The sum of relative populations in aqueous phase was 50.20 % for a_{CT}, 48.60 % for b_{CT}, and 1.20 % for c_{CT}. Therefore, when including aqueous solvent, the populations of both b_{CT} and

Table 1 Electronic energy calculated at the B3LYP/6-31G(d,p) level of theory, corrected by zero point energy (ZPE), and characteristic dihedral angle τ of different minimum energy conformers of (4α→6″, 2α→*O*→1″)-phenylflavan a_{CT}, b_{CT}, and c_{CT} in gas phase, and in polarizable continuum model (PCM)-simulated aqueous solution

Conformer	Rotamer	Vacuum					Solution					
		Angle τ	Energy (kcal mol^{-1})	ΔE [a] (kcal mol^{-1})	ΔE [b] (kcal mol^{-1})	Relative population (%)[c]	Angle τ	Energy (kcal mol^{-1})	ΔE [a*] (kcal mol^{-1})	ΔE [b*] (kcal mol^{-1})	ΔE [c*] (kcal mol^{-1})	Relative population (%)[d]
$a1_{CT}$	Z_1	87.39	−791,229.985	0.17	0.17	19.41	87.62	−791,242.213	12.23	0.04	0.04	22.36
$a3_{CT}$	Z_2	183.16	−791,228.559	1.59	1.59	1.75	179.91	−791,240.915	12.36	1.34	1.34	2.50
$a2_{CT}$	Z_1	269.18	−791,230.151	0.00	0.00	25.73	270.59	−791,242.257	12.11	0.00	0.00	24.09
$a4_{CT}$	Z_2	3.48	−791,227.706	2.45	2.45	0.41	2.06	−791,240.504	12.80	1.75	1.75	1.25
$b1_{CT}$	Z_1	90.10	−791,229.702	0.45	0.09	12.05	90.83	−791,242.227	12.53	0.03	0.00	22.92
$b3_{CT}$	Z_2	183.86	−791,227.946	2.21	1.85	0.62	177.21	−791,240.584	12.64	1.67	1.64	1.43
$b2_{CT}$	Z_1	264.96	−791,229.792	0.36	0.00	14.02	270.62	−791,242.207	12.41	0.05	0.02	22.13
$b4_{CT}$	Z_2	0.90	−791,227.876	2.28	1.92	0.55	1.49	−791,240.818	12.94	1.44	1.41	2.12
$c1_{CT}$	Z_1	85.78	−791,225.919	4.23	0.06	0.02	87.47	−791,239.971	14.05	2.29	0.10	0.51
$c3_{CT}$	Z_2	182.76	−791,224.346	5.81	1.63	0.00	179.73	−791,238.754	14.41	3.50	1.32	0.06
$c2_{CT}$	Z_1	267.45	−791,225.980	4.17	0.00	0.02	271.30	−791,240.075	14.10	2.18	0.00	0.60
$c4_{CT}$	Z_2	4.06	−791,223.655	6.50	2.32	0.00	2.89	−791,238.297	14.64	3.96	1.78	0.03

[a] Energy difference solution − vacuum

[b] Energy difference relative to the most stable conformer

[c] Energy difference relative to the most stable conformer in each group

[d] Relative population percentage calculated according to Maxwell-Boltzmann distribution at 298.15 K, expressed in % [*energy calculated at B3LYP/6-31G(d,p) corrected by zero point energy (ZPE)]

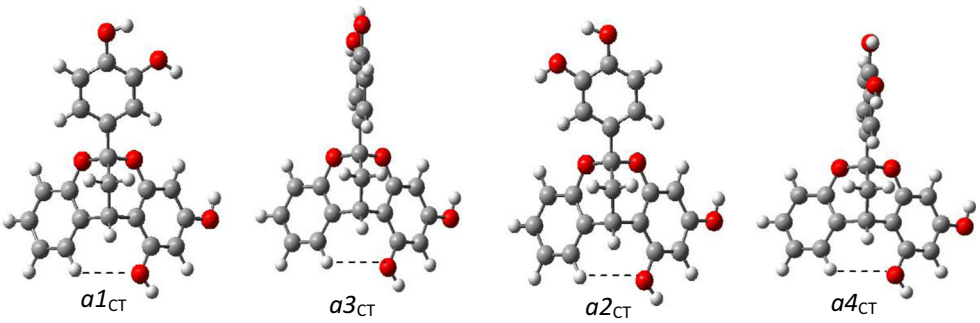

Fig. 2 Optimized geometries of Z_1 isomers of (4α→6″, 2α→*O*→1″)-phenylflavan substituted with R′=R=OH calculated under vacuum at the B3LYP/6-31G(d,p) level of theory. *Dotted lines* Intramolecular hydrogen bond (HB) interactions

c_{CT} conformers increased at the expense of decreasing the a_{CT} population.

The structural parameters of optimized structures in solution showed small changes from the values under vacuum. Variations in some geometric parameters of the conformers under study due to aqueous solvent effect are shown in Table S2 (Supplementary Material).

In phenylflavan substituted with R′=R=OH, a difference of up to 3.00°, similar to R′=H, R=OH substitution (3.30°) [11], was observed for the dihedral angles that define the position of ring B with respect to the A–C conjugated system (C3—C2—C1′—C2′ and C3—C2—C1′—C6′ dihedral angles) in solution. The position of the OH groups of the catechol and resorcinol rings was not significantly changed. Instead, the variation thereof was about 14.0° for (+)-catechin [12]. Therefore, except for (+)-catechin [12], solvent slightly affects the ring B position relative to the A–C system.

Intramolecular HB interactions in the catechol ring

As previously reported for (+)-catechin [12], intramolecular HB interactions in the catechol ring could not be characterized by charge density topology using standard search criteria for BCPs. However, HB occurrence in the catechol ring has been widely documented [23–25], although characterizations by AIM theory were not reported in any of these latter reports. On the contrary, in the phenylflavan substituted with R′=R=OH, and in (+)-catechin [12], these interactions can be characterized by geometric criteria, e.g., an O3′···H4′ distance of 2.127 Å, and O3′···H4′—O4′ angle of 114.44° for *a1* structures, and O4′···H3′ distance of 2.128 Å, and O4′···H3′—O3′ angle of 114.44° for *b1*. Therefore, the intramolecular HB interaction in the catechol ring of *a1* structures can be considered as stronger than that in *b1*.

Also, the occurrence of a charge transfer between oxygen lone pairs and the $1n_O \rightarrow \sigma^*_{O-H}$ hydroxyl antibonding orbital, typical of HB interactions, was revealed by NBO analysis, being only slightly more effective for *a1* than for *b1*. Second-order stabilization energy $E^{(2)}$ values were 0.98 kcal mol^{-1} and 0.96 kcal mol^{-1}, respectively, which was in agreement with the shortest distance of the former structure.

The presence of solvent affected HB interactions slightly. The O···H distances did not vary appreciably (on average, a 0.03 % decrease). The O···OH angle decreased on average by 0.3 %. (Table S3; Supplementary Material). Variations were similar to those reported for (+)-catechin [12].

The $1n_O \rightarrow \sigma^*_{O-H}$ charge transfer increased 4.67 % on average. The NBO analysis showed that such transfer was slightly more effective in *b2* than in *a1*, second-order stabilization energy $E^{(2)}$ values being 1.02 kcal mol^{-1} and 1.01 kcal mol^{-1}, respectively.

These findings demonstrated the presence of HB interactions in the catechol ring of both *a* and *b* structures, thus explaining the greater stability of these two conformers compared to *c*-type structures. The stabilizing effect of these HB interactions was 4.00 kcal mol^{-1} on average, calculating the energy difference between *a1* and *b1* conformers, and *c1* conformers (Table S4; Supplementary Material).

The mean energy difference between structures with HB in the catechol ring (*a* and *b* structures), and those without (*c* structures) was 2.20 kcal mol^{-1} in an aqueous solvent. The smallest difference found in solution, even when HB interactions were stronger, was due to the higher stabilization of *c* structures (approximately 3.00 kcal mol^{-1}) in aqueous solvent (Table 1), similar to that reported for (+)-catechin [12] (approximately 2.00 kcal mol^{-1}).

MEP analysis can efficiently identify the presence of intramolecular HB interactions, as previously reported [10, 12]. In the present case, this analysis tool also confirmed the occurrence of O···H—O intramolecular HB interactions in the catechol ring of phenylflavan substituted with R′=R=OH, as reported for (+)-catechin [12]. In fact, the MEP of the *a1* conformer showed that the V(r) value on the HB-involved O atom (atom of the H acceptor portion) became less negative (higher) than the V(r) of the atom not involved in this interaction (e.g., $\Delta_{O3'\text{-}O4'} \cong 15.3$ kcal mol^{-1}). The positive V(r) value on the HB hydrogen atom (belonging to the H donor portion) became more negative (lower) than on any other hydrogen (e.g., $\Delta_{H\neq 4'\text{-}H4'} \cong 23.0$ kcal mol^{-1}). The V(r) value on the atom of the donor portion decreased, while V(r) on the acceptor increased (Fig. 3). V(r) variations caused by solvent effect on O and H atoms involved in intramolecular interactions were

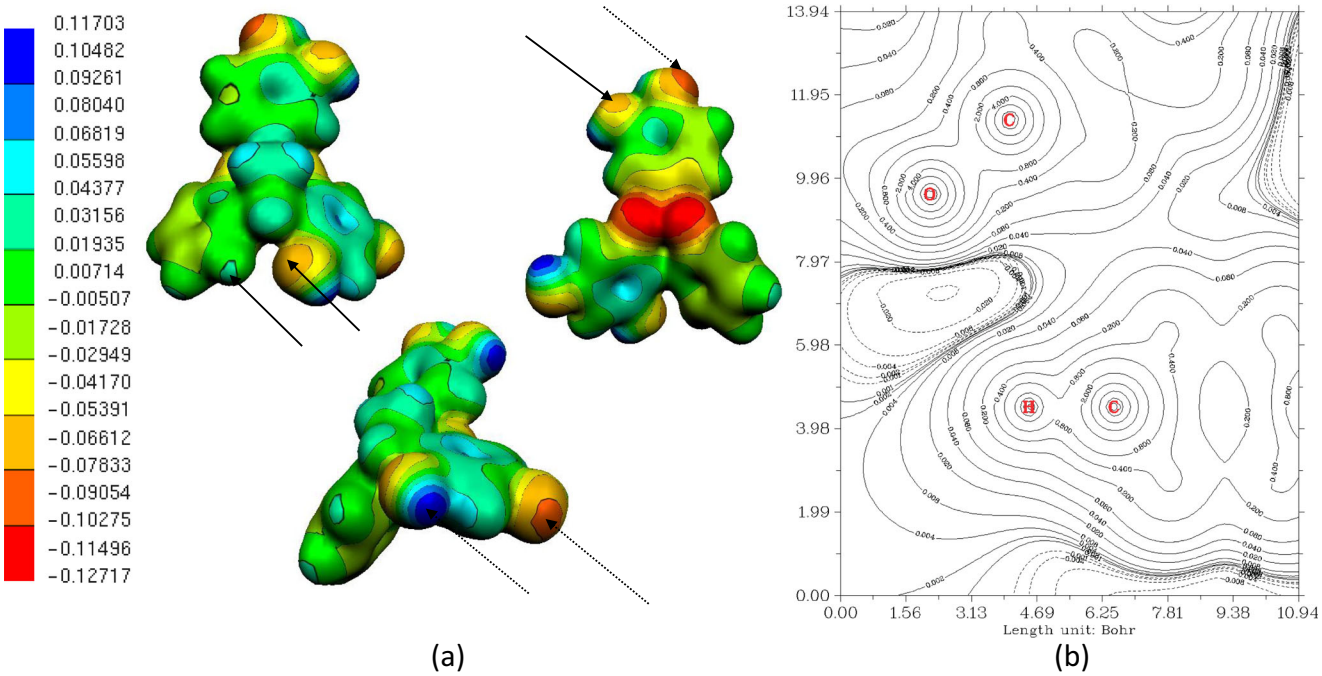

Fig. 3 **a** Molecular electrostatic potential (MEP) on van der Waals surface for *a1* structure in vacuum, showing modification of the positive V(r) value on hydrogen atoms, and the negative V(r) value on hydroxyl oxygen atoms involved or not in an intramolecular HB. *Solid lines* Atoms involved in the interaction, *dotted lines* atoms not involved in the interaction. **b** MEP contours for *a1* structure in vacuum accounting for the plane of the HB interaction relative to an OH group of the resorcinol ring

lower than those of (+)-catechin (17.0 kcal mol^{-1} and 33.0 kcal mol^{-1}, respectively [12]).

Intramolecular HB interactions in the resorcinol ring

In phenylflavan substituted with R′=R=OH, the H···O intramolecular HB interactions were also characterized between the HO-5″ oxygen atom of the resorcinol ring, and the H-5 atom of ring A. These interactions are shown as dotted lines in Fig. 2.

Relevant geometric parameters of these interactions, such as H···O, C···O distances, and C—H···Y bond angles, Y = O, are shown in Table S5 (Supplementary Material). Local topological properties calculated in the respective BCP are shown in Table S6 (Supplementary Material).

The H···O bonds were found in all conformers, with a mean H···O distance of 2.94 Å (within the expected range of 2.0–3.0 Å for C—H···O bonds, with C as "D" donor atom of hydrogen, and O as "A" acceptor atom: D—H···A). As already reported [26], the shorter the H···A interatomic distance, and closer to 180.0° the D—H···A angle became, the greater the strength of the HB interaction. Another parameter that characterized such bonds as weak HBs was the distance between the C atom bonded to the H that formed the bridge, and the O atom (mean values of 3.54 Å) [26]. The bond angle between donor and acceptor atoms (C—H···O) varied in the range of 114.7–115.0°. Electron density values were lower than those expected for typical intramolecular HB (expected electron density around 0.02–0.03 a.u.) [27, 28]. Given the correlation between the density in BCP and interaction strength [29], this interaction was also typically weak from the analysis of the topological parameters, contributing very little to structure stabilization. $\nabla^2\rho_b$ varied in the range of 0.002–0.016 a.u., and ellipticity, ε, between 0.271 and 0.294. As a result, these intramolecular interactions in the resorcinol ring were stronger than those described for phenylflavan substituted with R′=H, R=OH, but with high ε values [10].

Solvent slightly affected HB interactions. The O···H distances did not vary appreciably (on average a 0.3 % increase). The O···OH angle decreased on average by 0.4 %.

MEP analysis revealed the occurrence of O···H intramolecular HB in the resorcinol ring as for other compounds of the series. The V(r) value on the atom of the acceptor portion increased, while V(r) decreased on the donor portion. These results were in agreement with the electrostatic potential complementarity between the positive region of the hydrogen atom of the H donor, and the negative region of the H acceptor in intermolecular HBs [29]. The MEP of the *a1* conformer showed that the V(r) value on the HB oxygen atom (atom of H acceptor portion) became less negative (higher) than the V(r) of the atom that was not involved in the HB interaction (e.g., $\Delta_{O3''\text{-}O5''} \cong 15.3$ kcal mol^{-1}). The positive V(r) value on the H atom of the O···H HB (donor portion, C—H) became more negative (smaller) than on another aromatic H atom

(e.g., $\Delta_{H\neq 5\text{-}H5} \cong 30.6$ kcal mol^{-1}) (Fig. 3). The V(r) value on the donor portion atom decreased, while V(r) on the acceptor portion increased.

AIM and NBO electronic structural analysis

The most significant local topological properties in BCPs [e.g. electron charge density in BCP (ρ_b), Laplacian of electron charge density ($\nabla^2\rho_b$), three eigenvalues of the Hessian matrix (λ_1, λ_2, and λ_3), ellipticity (ε), relationship between the perpendicular and parallel curvature ($|\lambda_1|/\lambda_3$), and kinetic energy density per charge unit (G_b/ρ_b)], of the chemical bonds of the most stable a_{CT} and b_{CT} conformers are shown in Tables S7 and S8 (Supplementary Material), both in gas phase and in a simulated aqueous solvent. Polar covalent interactions and intermediate polar covalent interactions were characterized by the redistribution of charge density on the adjacent molecular region as previously reported for compounds of the series [9–12].

The ε values (bond π character) were higher in substituted rings (Table 2), further decreasing on average as follows, ring D > ring B > ring A > benzene, thus indicating increased π electron availability in ring D, as previously reported for phenylflavan substituted with R′=H, R=OH [11]. Accordingly, the resorcinol ring would have greater π-electron availability than the catechol ring. Similar results were found for (+)-catechin, e.g., ellipticity values obtained by averaging over rings B and A bonds of Z_1 conformers were 0.247 and 0.273, respectively (values not previously reported).

The sums of the second order stabilization energies $E^{(2)}$ by NBO analysis that describe the effects of charge delocalization, and explain the greater stability of Z_1 rotamers over Z_2 are shown in Table 3. Electron charge transfers from and to the bonds of ring C, as well as O and O-1 lone pair transfers of this ring, play an important role in stabilizing both rotamers. Consequently, despite being non-planar structures, ring B was not independent of ring A, as reported for other similar compounds [9–12].

Due to the higher stability of Z_1 rotamers than Z_2, four Z_1 structures of *a* and *b* groups, namely *a1*, *a2*, *b1* and *b2*, were selected for further analysis.

It can be concluded from Table 3 that all conformers of the structures under study showed nearly the same second order stabilization energies for $1n_{O1}\rightarrow\sigma^*_{C8a-C8}$ transfer (0.56 - kcal mol^{-1} on average). In addition, energies associated with $1n_{O1}\rightarrow\sigma^*_{C8a-C4a}$ and $2n_{O1}\rightarrow\pi^*_{C8a-C4a}$ transfers were, on average, 7.09 kcal mol^{-1} and 25.69 kcal mol^{-1}, respectively, resulting in lower values than in phenylflavan substituted with R′=H, R=OH [10]; this in turn is lower than in the phenylflavan substituted with R′=R=H (0.56 kcal mol^{-1}, 7.15 kcal mol^{-1}, and 26.30 kcal mol^{-1}, respectively) [9].

Hyperconjugative interactions related to the O atom were $1n_O\rightarrow\sigma^*_{C1''-C2''}$ (0.54 kcal mol^{-1} on average), $1n_O\rightarrow\sigma^*_{C1''-C6''}$ (6.74 kcal mol^{-1}), and $2n_O\rightarrow\pi^*_{C1''-C2''}$ (27.46 kcal mol^{-1}), thus describing the resonance of the oxygen lone pairs with rings A and D.

Bond polarization by NBO calculations determined the percent electron density on each bond atom (Table S9; Supplementary Material). Therefore, C2—C3 polarization was greater than that of C3—C4 in the phenylflavan substituted with R′=R=OH, as previously reported for similar compounds [10].

In addition, the C2—C3 bond was more polarized in phenylflavan substituted with R′=R=OH (on average 49.26 % on C-2, and 50.74 % on C-3), than when substituted with R′=R=H, and with R′=H, R=OH (49.35 % on C-2, and 50.65 % on C-3).

The conjugative and hyperconjugative interactions of O and O-1 oxygen lone pairs explained the increase of the positive eigenvalue of the Hessian matrix (λ_3 curvature) at critical points (CPs), and the distinctive topological features of C8a—O1 bond compared to C2—O1 (and C1″—O against C2—O) mentioned above, and previously reported for all similar compounds [9, 11]. This behavior was associated with a greater charge concentration on C-8a and C-1″ atoms than on C-2 (119.62 a.u. at CNP for C-8a, and C-1″ against 119.54 a.u. at CNP for C-2).

As for other similar compounds [9, 11], the weakness of C3—H and C4—H compared to the other C—H bonds of rings A, B, and D was associated with the donor role in hyperconjugative interactions, and explained the ε increase at BCP of the bonds that connected them with the rest of the structure (C2—C3 and C3—C4 bonds), thus further indicating a slight π character of these simple bonds (Tables S7 and S8; Supplementary Material). There were also transfers that explained the loss of symmetry for ring A compared to benzene (Table 4), being associated with ε values of some bonds, and mechanisms by which O-1 donated electron density to ring A (charge density increase on C-5 and C-7 atoms, e.g., 119.620 a.u., 119.604 a.u., 119.627 a.u., 119.605 a.u., 119.622 a.u., and 119.605 a.u. for C-8a, C-4a, C-5, C-6, C-7, and C-8 atoms, respectively).

In Z_1 structures C1′—C2′ (1.399 Å), C1′—C6′ (1.399 Å), C3′—C4′ (1.398 Å), and C4′—C5′ (1.401 Å), bonds were longer than the other ring B bonds (1.396 Å). These bonds also showed higher ellipticity (0.220–0.290 range) than typical aromatic bonds ($\varepsilon = 0.200$), as previously reported for (+)-catechin. Similar behavior was observed for Z_2 compounds.

NBO analysis revealed significant charge transfers from the C2—C1′ bonding orbital to the C1′—C2′ and C1′—C6′ antibonding orbitals (Table S10; Supplementary Material). Moreover, transfers were also found from C2—O, C2—O1, O3′—H, and O4′—H bonding orbitals to C1′—C2′, C1′—C6′, C3′—C4′, and C4′—C5′ antibonding orbitals (Tables 3 and Table S10; Supplementary Material). These charge transfers explained the greater length of the bonds mentioned above.

Table 2 Values of mean ellipticity (ε) for bonds of each ring calculated at the B3LYP/6-311++G(d,p) level of theory in vacuum for different substitutions of rings A, B, and D of Z_1 conformers. Percentage variations in PCM-simulated aqueous solution are also reported

Substituent	Vacuum			Percentage variation in solution		
	R′=H, R=H	R′=H, R=OH	R′=OH, R=OH	R′=H, R=H	R′=H, R=OH	R′=OH, R=OH
Ring A	0.223	0.223	0.222	−1.44	−1.35	−0.90
Ring B	0.203	0.203	0.246	−1.70	−1.57	−1.22
Ring D	0.223	0.272	0.273	−1.44	−0.74	−0.73

Analysis of the hyperconjugative interactions among different rings showed the existence of electron charge delocalization mechanisms acting cooperatively as "delocalization routes", showing interactions occur between rings even when not sharing the same plane. Charge transfers, and $E^{(2)}$ values are shown in Fig. 4. Values obtained for the phenylflavan substituted with R′=H, R=OH, and (+)-catechin are also shown. The results indicated that these “delocalization routes” were more effective for the phenylflavan substituted with R′=R=OH than for (+)-catechin. All these results are relevant for further study of the molecular basis of the different antioxidant mechanisms proposed in the literature.

Aqueous solvent effects on AIM-NBO electron structure analysis

As reported for other compounds of the series [9–12], the AIM characterization of atomic interactions in gas phase underwent small variations due to the inclusion of the aqueous solvent [Tables S7 and S8; Supplementary Material, topological parameters for CPs (3, −1)].

There were also changes at CPs (3, −3) or CNP in solution. Concerning aromatic H atoms, there was an electron density decrease at CNP, not exceeding 1.1 %. However, CNP values of hydroxyl H atoms decreased as much as 4.0 % compared to gas phase.

Table 3 Second order energies $E^{(2)}$ associated with charge transfers that explain the higher stability of Z_1 rotamers compared to Z_2 in gas phase, calculated at the B3LYP/6-311++G(d,p) level of theory. Values are expressed in kcal mol^{-1}

		a_{CT}				b_{CT}			
		Z_1		Z_2		Z_1		Z_2	
Donor	Acceptor	$a1_{CT}$	$a2_{CT}$	$a3_{CT}$	$a4_{CT}$	$b1_{CT}$	$b2_{CT}$	$b3_{CT}$	$b4_{CT}$
$\sigma_{O1–C2}$	$\sigma^*_{C1'–C6'}$	1.99	1.96	1.52	1.50	1.86	1.88	1.49	1.41
$\sigma_{O–C2}$	$\sigma^*_{C1'–C2'}$	1.93	1.97	1.30	1.28	1.89	1.87	1.22	1.34
	∑	3.92	3.93	2.82	2.78	3.75	3.75	2.71	2.75
$\sigma_{C2–C1'}$	$\sigma^*_{C8a–O1}$	2.58	2.59	2.68	2.68	2.59	2.59	2.68	2.70
	$\sigma^*_{O–C1''}$	2.62	2.60	2.74	2.75	2.59	2.60	2.74	2.74
	$\sigma^*_{C2–C3}$	0.96	0.95	0.93	0.93	0.95	0.95	0.93	0.93
	$\sigma^*_{C3–C4}$	1.63	1.64	1.35	1.4	1.65	1.64	1.35	1.34
	∑	7.79	7.78	7.70	7.76	7.78	7.78	7.7	7.71
$1n_{O1}$	$\sigma^*_{C8a–C8}$	0.55	0.56	0.54	0.55	0.56	0.55	0.55	0.55
	$\sigma^*_{C8a–C4a}$	7.08	7.08	7.03	7.05	7.09	7.08	7.05	7.05
	$\sigma^*_{C2–C3}$	3.99	4.10	4.01	4.04	4.04	4.06	4.02	4.05
	∑	11.62	11.74	11.58	11.64	11.69	11.69	11.62	11.65
$1n_{O}$	$\sigma^*_{C2''–C1''}$	0.54	0.53	0.51	0.54	0.54	0.54	0.51	0.54
	$\sigma^*_{C1''–C6''}$	6.74	6.74	6.70	6.97	6.74	6.75	6.72	6.98
	$\sigma^*_{C2–C3}$	3.77	3.69	3.71	3.71	3.77	3.75	3.71	3.73
	∑	11.05	10.96	10.92	11.22	11.05	11.04	10.94	11.25
$1n_{O1}$	$\sigma^*_{C2–C1'}$	0.84	0.83	0.82	0.81	0.85	0.82	0.82	0.8
$1n_{O}$	$\sigma^*_{C2–C1'}$	0.83	0.83	0.78	0.77	0.83	0.86	0.77	0.78
	∑	1.67	1.66	1.60	1.58	1.68	1.68	1.59	1.58
	$\sum_{TOTAL}$	36.05	36.07	34.62	34.98	35.95	35.94	34.56	34.94

Table 4 Percentage values of the main changes in second order energies $E^{(2)}$ calculated at the B3LYP/6-311++G(d,p) level of theory for relevant electronic charge transfers from oxygen lone pairs of (4α→6″, 2α→*O*→1″)-phenylflavan substituted with R′=R=OH in PCM-simulated aqueous solution

Donor	Acceptor	$a1_{CT}$	$a2_{CT}$	$b1_{CT}$	$b2_{CT}$
$1n_{O1}$	$\sigma^*_{C8—C8a}$	−3.57	−3.64	−3.64	−3.57
$1n_{O1}$	$\sigma^*_{C4a—C8a}$	−0.28	−0.42	−0.14	−0.42
$2n_{O1}$	$\pi^*_{C4a—C8a}$	−1.99	−2.53	−2.10	−2.18
$1n_{O}$	$\sigma^*_{C1''— C6''}$	−1.78	−1.78	−1.78	−1.63
$1n_{O}$	$\sigma^*_{C1''—C2''}$	−3.77	−5.56	−3.70	−5.56
$2n_{O}$	$\pi^*_{C1''—C2''}$	−4.89	−5.05	−5.05	−4.81
$1n_{O1}$	$\sigma^*_{C2—C1'}$	−6.02	−4.88	−7.32	−7.06
$2n_{O1}$	$\sigma^*_{C2—C1'}$	−1.63	3.28	0.82	0.00
$1n_{O}$	$\sigma^*_{C2—C1'}$	−2.41	−2.41	−2.33	−3.61
$2n_{O}$	$\sigma^*_{C2—C1'}$	6.59	−2.15	1.05	2.06
$1n_{O1}$	$\sigma^*_{C2—C3}$	7.05	−8.62	0.00	−0.53
$2n_{O1}$	$\sigma^*_{C2—C3}$	−4.52	−7.74	−7.01	−5.10
$2n_{O1}$	$\sigma^*_{C2—O}$	−3.77	−2.39	−3.95	0.00
$1n_{O3''}$	$\sigma^*_{C2''—C3''}$	3.55	3.40	3.56	3.70
$2n_{O3''}$	$\pi^*_{C3''— C4''}$	1.32	1.03	1.42	1.14
$1n_{O5''}$	$\sigma^*_{C4''—C5''}$	5.25	5.43	5.43	5.60
$2n_{O5''}$	$\pi^*_{C5''— C6''}$	8.27	8.28	8.31	8.23
$1n_{O3'}$	$\sigma^*_{C—C,O—H/C3'—C4'}$	6.35	6.22	6.48	6.24
$2n_{O3'}$	$\pi^*_{C2'— C3'}$	8.27	8.28	8.31	8.23
$1n_{O4'}$	$\sigma^*_{C3'—C4'/\sigma^*C—C,O—H}$	0.00	0.00	−0.32	−0.16
$2n_{O4'}$	$\pi^*_{C4'— C5'}$	−2.10	−2.18	−2.12	−2.01

[a] Values are expressed in kcal mol^{-1}

The inclusion of the aqueous solvent resulted in a decrease in the mean bond ellipticity of different rings. The effect was more pronounced for ring B (Table 2), as in (+)-catechin (in solution, −1.42 % variation for ring B, and −1.06 % for ring A). This decrease was modulated in the phenylflavan by the substituents, and was attenuated in the following order, R′=R=H>R′=H, R=OH>R′=R=OH. Also in solution, the mean bond ellipticity was greater for ring D than for ring B, as reported for (+)-catechin [12]. The ε values showed that, also in solution, the bond π character decreased on average in the following order, ring D > ring B > ring A > benzene.

From the NBO analysis, the two lone pairs for each O atom were characterized both in vacuum and in solution. One of them (*1n*) was *sp*-type, and the other one (*2n*) was *p*-type, each playing a different role. Also, in solution, substitution of ring D led to a higher polarization of the C2─C3 bond than that of C3─C4; the difference was even more pronounced (Table S9; Supplementary Material).

Besides these similarities, there were interesting changes in electron delocalizations in solution.

The main changes in second order stabilization energy (x) of the relevant charge transfers, e.g., $1,2n_{O,\ O1}\rightarrow\sigma^*, \pi^*$ ($\%\Delta_{\sigma\rightarrow\sigma^*}$ and $\%\Delta_{1,2nO,\ O1\rightarrow\sigma^*,\ \pi}$, respectively), and σ→σ * are shown in Tables 4 and 5 in terms of percent.

Some variations were as follows:

(1) Both in solution and in vacuum, the $\sigma_{C3—H}\rightarrow\sigma^*_{C—O}$ transfer was higher than that of $\sigma_{C3—H}\rightarrow\sigma^*_{C—C}$. Furthermore, both types of delocalizations increased in solution, e.g., transfer to C─O antibonding orbital increased 3.7–4.7 %, and transfer to C─C antibonding orbital increased 1.1–2.3 % (Table 5).

(2) Second order stabilization energies for $\sigma_{O3''—H}\rightarrow\sigma^*$ and $\sigma_{O5''—H}\rightarrow\sigma^*$ transfers increased up to 3.1 % in solution (Table 5).

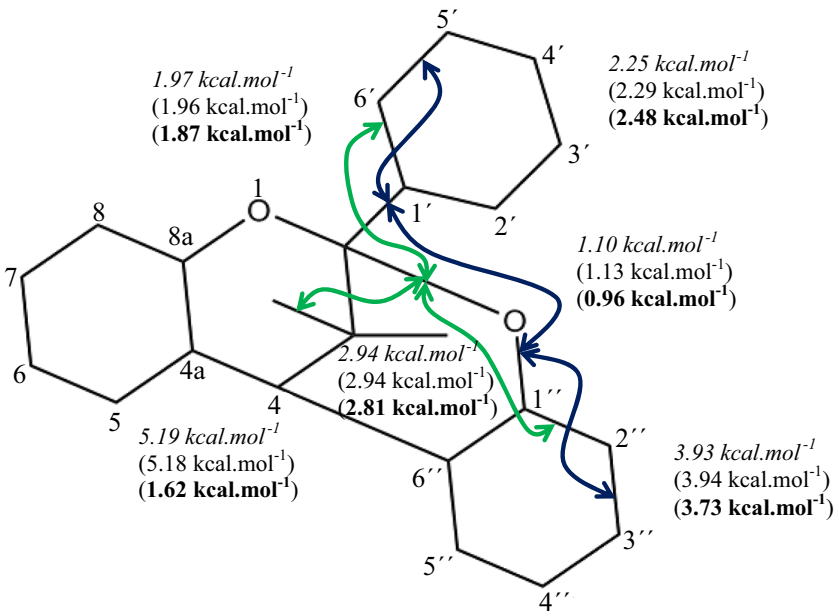

Fig. 4 Values of second order energies $E^{(2)}$ accounting for charge transfers associated with "delocalization routes" in (4α→6″, 2α→*O*→1″)-phenylflavan substituted with R′=R=OH calculated in vacuum at the B3LYP/6-311++G(d,p) level of theory. Values obtained for (4α→6″, 2α→*O*→1″)-phenylflavan substituted with R′=H, R=OH, and (+)-catechin are indicated in *brackets*, the latter being in *bold*

Table 5 Percentage values of the main changes in second order energies $E^{(2)}$ calculated at the B3LYP/6-311++G(d,p) level of theory for relevant electronic charge transfers in (4α→6″, 2α→*O*→1″)-phenylflavan substituted with R′=R=OH in PCM-simulated aqueous solution.[a,b]

Donor	Acceptor	a_{CT}	b_{CT}
σ_{C3-H}	$\sigma^*_{C4-C6''}$	1.13	1.13
σ_{C3-H}	σ^*_{C2-O}	3.66	3.75
σ_{C3-H}	σ^*_{C4-C4a}	2.12	2.31
σ_{C3-H}	σ^*_{C2-O1}	4.71	4.73
$\sigma_{O3''-H}$	σ^*_{C-C}[c]	0.49	0.39
$\sigma_{O5''-H}$	σ^*_{C-C}[c]	2.95	3.07
$\sigma_{C2-C1'}$	$\sigma^*_{C1'-C6'}$	−0.76	2.12
$\sigma_{C2-C1'}$	$\sigma^*_{C1'-C2'}$	0.00	1.67
$\sigma_{C2-C1'}$	$\sigma^*_{C5'-C6'}$	−0.74	−3.04
$\sigma_{C2-C1'}$	$\sigma^*_{C2'-C3'}$	0.22	−0.82
$\sigma_{C5'-C6'}$	$\sigma^*_{C4'-O}$	3.22	−42.00
$\sigma_{C2'-C3'}$	$\sigma^*_{C4'-O}$	1.46	61.68
σ_{C2-C3}	$\sigma^*_{C1'-C2'}$	3.85	0.00

[a] Values are expressed in kcal mol^{-1}

[b] Average values for all conformers of (4α→6″, 2α→*O*→1″)-phenylflavan substituted with R′=R=OH

[c] C─C accounts for bonds of ring D

(3) Charge transfers from O-3″ and O-5″ lone pairs to the antibonding orbitals of ring D increased from 3.7 % to 5.6 % in solution (Table 4) due to hybridization. In solution, the *p* character of *1n* lone pair bonding orbitals increased (up to 3.0 %). Therefore, it was proposed that the best O-3″ and O-5″ delocalizations were based on the solvent effect on lone pair hybridization. The *p* character increase of *1n* lone pairs allowed a better overlap between them and the C─C antibonding orbitals of ring D (Table S11; Supplementary Material).

(4) The O and O-1 lone pairs showed a different behavior. Transfers of these lone pairs in Z_1 isomers decreased up to 8.6 % in solution (Table 4). Second order stabilization energies for $1n_{O1}\rightarrow\sigma^*_{C8-C8a}$ transfer, and symmetrical equivalent ($1n_{O}\rightarrow\sigma^*_{C1''-C2''}$) decreased 3.6–5.6 % in Z_1 isomers.

(5) In relation to the decrease of hyperconjugative interactions of $1n_{O,O1}\rightarrow\sigma^*_{C2-C1'}$ oxygen lone pairs in solution (Table 4), and $\sigma_{C2-C1'}\rightarrow\sigma^*_{C5'-C6'}/\sigma^*_{C2'-C3'}$ transfers were both found to diminish (Table 5). These findings were related to the decrease in mean bond ellipticities of ring B, and may explain the π character decrease of ring B in terms of the reduction in charge delocalization effects referred to O-1 and O lone pairs in solution (anomeric effect).

(6) Aqueous solvent resulted in variations for some transfers in vacuum for the catechol ring. Although these variations were very similar to those found in (+)-catechin, they were all attenuated by R′=R=OH substitution. This trend was consistent with the lowest stabilization in solution of the compound analyzed herein.

Table 6 Percentage values of the main changes in second order energies $E^{(2)}$ calculated at the B3LYP/6-311++G(d,p) level of theory for relevant electronic charge transfers from π orbitals of C2′─C3′ and C4′─C5′ bonds of (4α→6″, 2α→*O*→1″)-phenylflavan substituted with R′=R=OH in PCM-simulated aqueous solution[a]

Donor	Acceptor	$a1_{CT}$	$a2_{CT}$	$b1_{CT}$	$b2_{CT}$
$\pi^*_{C2'-C3'}$	$\pi^*_{C1'-C6'}$	2.81	3.36	5.44	5.38
	$\pi^*_{C2'-C3'}$	3.06	2.33	4.54	4.24
$\pi^*_{C4'-C5'}$	$\pi^*_{C1'-C6'}$	−2.24	−2.23	−3.59	−3.07
	$\pi^*_{C4'-C5'}$	−3.77	−3.33	−5.33	−4.67

[a] Values are expressed in kcal mol^{-1}

These variations were similar to those found for phenylflavan substituted with R′=H, R=OH, although attenuated by the R′=R=OH substitution.

Regarding the decrease in hyperconjugative interactions of $2n_{O4'}\rightarrow\pi^*_{C4'-C5'}$ oxygen lone pairs in solution (Table 4), $\pi_{C4'-C5'}\rightarrow\pi^*_{C-C}$ transfers were also decreased (Table 6). On the contrary, increasing $2n_{O3'}\rightarrow\pi^*_{C2'-C3}$ oxygen lone pair hyperconjugative interactions in solution (Table 4) was related to an increase in $\pi_{C2'-C3'}\rightarrow\pi^*_{C-C}$ transfer (Table 6), also proving the existence of delocalization routes, some of which being reinforced in solution.

Aqueous solvent effects on MEP and reactivity by AIM-NBO study

The procedure proposed by Politzer et al. [30] was used herein to predict susceptible sites to electrophilic attack in the region of negative V(r) values. The most stable structures were studied, as previously reported for similar compounds [9–12].

Results showed that the most reactive sites were located on the oxygen atoms (Fig. 5). The highest V(r) value (positive) showed an average increase of 33.46 % in solution, and the minor value (negative) a decrease of 18.77 % by comparison of the maximum and minimum V(r) values in both media, A similar variation was reported for (+)-catechin, being much greater for the phenylflavan substituted with R′=H, R=OH (46.99 % and −26.66 %) and R′=R=H (39.12 % and −31.14 %) (Table 7).

The greater reactivity of the phenylflavan substituted with R′=R=OH in aqueous solution rather than in vacuum is shown in Table 7. The phenylflavan substituted with R′=R=OH was more reactive than that substituted with R′=H, R=OH in gas phase, while the opposite behavior was found in solution. Consequently, a polar solvent such as water affected the structures differently, and the OH substitution of ring B (catechol ring) attenuated the effects of the aqueous solvent.

The increase in the positive V(r) value on the hydroxyl H atoms of catechol and resorcinol rings in solution is shown in Fig. 5. This change can be rationalized by the increased donor character of these O─H bonds in solution relative to the gas

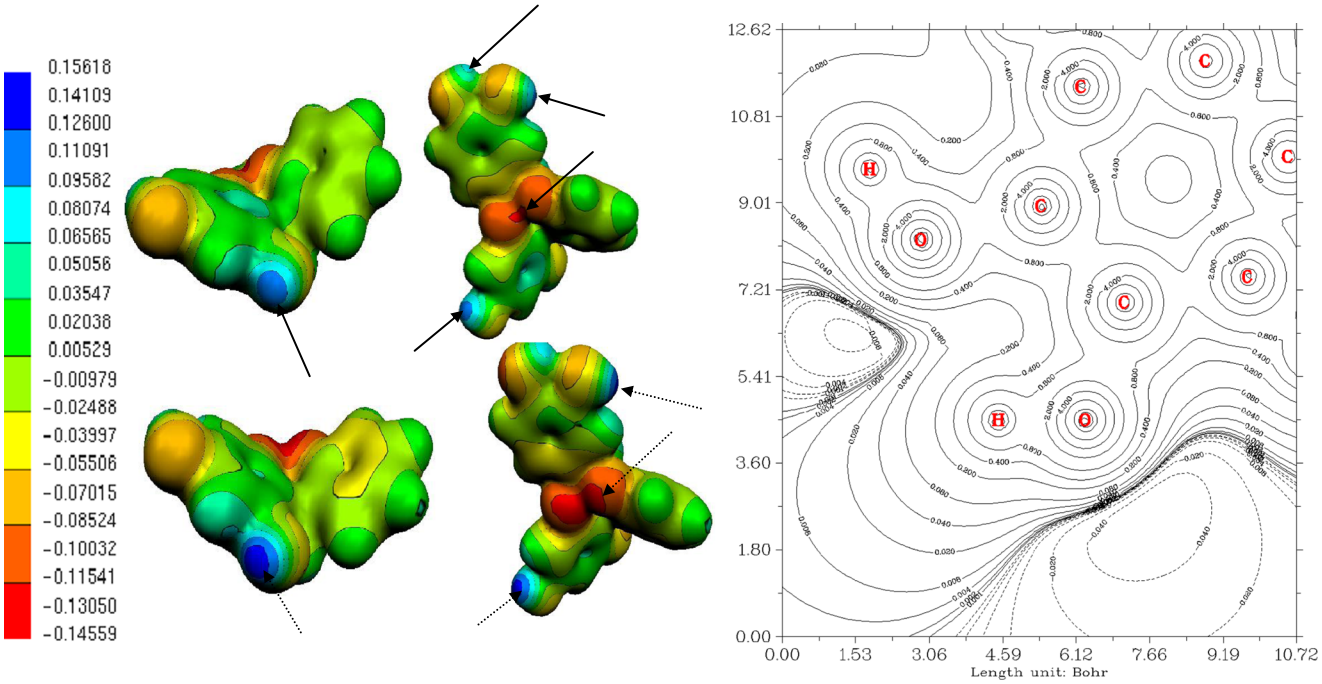

Fig. 5 **a** MEP on van der Waals surface for *a1*, where the modification of the positive V(r) value on hydroxyl H atoms, and the negative V(r) value on O atoms of rings C and B is observed. *Solid/dotted lines* are used to indicate areas of interest in vacuum/aqueous solution. **b** MEP contours for *a1* in vacuum accounting for the plane of the catechol ring, where the area of the HB interaction in such ring is observed

phase, which can be up to 5 % as shown in Table S12 (Supplementary Material). The previously reported decrease in CNP density of the H atoms in solution was also in agreement with this observation.

The $1n_{O3',O4'} \rightarrow \sigma^*_{O-H}$ charge transfer in solution was higher than that found in vacuum (on average 5.17 % increase). Moreover, charge transfers from the O and O-1 oxygen atoms of rings C and E usually decreased in solution. In *a1*, for example, the decrease expressed as percentage difference for $1,2n_O \rightarrow \sigma^*$, π^* transfers was −2.99 % [$\Delta_{Solvent\text{-}Vacuum}$ = (65.93–67.96) kcal mol^{-1}], and for $1,2n_{O1} \rightarrow \sigma^*$, π^* transfers was −1.65 % [$\Delta_{Solvent\text{-}Vacuum}$ = (23.25–23.64) kcal mol^{-1}].

A large area accounting for negative potential on oxygen atoms, whose donor role in solution decreased, is shown in Fig. 5. This indicated an increase in the reactivity of these sites. When the donor role increased, the opposite was observed. Therefore, increased V(r) negative values may be explained as a decreased donor role of O lone pairs as previously reported [11, 12].

Molecular polarizability and permanent electric dipole moment

Molecular polarizability, $<\alpha>$, and permanent electric dipole moment, μ, were also studied throughout the conformational

Table 7 Values of maximum and minimum V(r) molecular electrostatic potential in vacuum, and in PCM-simulated aqueous solution[a]

	R′=R=H		R′=H, R=OH		R′=H, R=OCH_3		(+)-catechin		R′=OH, R=OH	
	V_{max}	V_{min}	V_{max}	V_{min}	V_{max}	V_{min}	V_{max}	V_{min}	V_{max}	V_{min}
Vacuum	28.05	−82.08	72.65	−79.62	37.76	−84.85	71.97	−78.99	73.74	−79.80
Solution	39.02	−103.60	106.23	−99.94	45.64	−107.49	95.12	−92.74	98.00	−91.36
Δ[b] (%)	39.12	−31.14	46.99	−26.66	21.45	−26.68	34.57	−17.41	33.46	−18.77

[a] Values are expressed in kcal mol^{-1}

[b] Percentage difference

space analyzed. The $<\alpha>$ values are shown in Table S13 (Supplementary Material). The $<\alpha>$ value of the most stable conformer was 232.84 a.u. higher than that reported for (+)-catechin (175.97 a.u. [31]). When considering the conformational space consisting of 12 conformers, this value was 233.06 a.u., and there was low fluctuation throughout the conformational space (Table S13; Supplementary Material). The results indicated the soluble nature of such structures in polar solvents, and their ability to polarize other atoms or molecules. Mean polarizability values, although very similar, decreased in the following order, c1 > b1 > a1 (likewise for 2- and 3-type structures). Note the higher polarizability of *c* conformers, which explains their greater stability in solution, as reported for (+)-catechin [31].

The values of μ throughout the conformational space analyzed are shown in Table S14 (Supplementary Material).

Values ranging from 1.33 to 3.47 D showed that these compounds can fit with the environment on the basis of dipole–dipole interactions. To take into account the entire conformational space, a statistical average was performed at 298.15 K by the Maxwell-Boltzmann distribution in each Cartesian component of μ.

The calculated μ module value for the most stable conformer was 1.733 D (*a2*) (3.077 D for (+)-catechin [31]), whereas, when all conformers were considered at room temperature by the Maxwell-Boltzmann distribution, it turned out to be 1.481 D (0.876 D for (+)-catechin [31]); showing a decrease of 14.5 % (71.4 % for (+)-catechin) from the μ module value for the most stable conformer of the phenylflavan substituted with R′=R=OH. Usually, this property was overestimated when considering the value of the most stable conformer, except for the phenylflavan substituted with R′=H, R=OH, where it was underestimated [11].

The magnitudes and directions of μ can serve as a useful tool for conformational analysis [32] because they are sensitive to molecular size and shape, as proposed for the phenylflavan substituted with R′=H, R=OH [11]. However, the results obtained herein indicated that the μ module value varied over a wide range, which was similar for all three groups (1.733–3.444 D for *a* structures; 1.918–3.466 D for *b*, and 1.327–2.154 D for *c*). Therefore, in the phenylflavan substituted with R′=R=OH, this magnitude was not useful to distinguish conformers from each other. Similar behavior was reported for (+)-catechin [31]. In other types of flavonoids, changes in μ were observed due to small structural changes [25, 33].

As reported for similar compounds [31], it was very difficult to obtain a relationship between this descriptor and the biological activity without prior knowledge of the flavonoid arrangement inside the enzyme. This latter work reported a high flexibility of such structures, leading to a large conformational space and a large variation in the μ modulus values and directions. Our results show the importance of knowing the conformational space, and μ values for each conformer.

The μ modulus values were 3.444 D, 1.733 D, and 2.681 D for $a1_{CT}$, $a2_{CT}$, and $a1_{TC}$ structures, respectively. Therefore, μ modulus values were greater for clockwise-oriented OH groups of the catechol ring than for counterclockwise-oriented ring B HO substituents [Figure S5a,b; Supplementary Material]. Upon analyzing μ variations in the resorcinol ring, the μ modulus value was greater for counterclockwise-oriented HO groups (CT-type conformation) than for clockwise-oriented OH groups (TC conformation) (Figure S5a,c; Supplementary Material).

As expected, μ modulus values increased in aqueous solution (Table S15; Supplementary Material) as reported for the phenylflavan substituted with R′=H, R=OH [11], but the greater attenuation might be due to the lower stabilization in solution for the phenylflavan substituted with R′=R=OH (60.0 % for R′=H, R=OH substitution vs. 45.0 % for R′=R=OH).

The solvent effect was not uniform, as shown in (Table S15; Supplementary Material). The Z_1 conformers with a C3–C2–C1′–C6′ dihedral angle (τ) close to 270.0° (*a2* and *b2*) showed greater variations (45.1 and 40.6 %, respectively) than those with such dihedral angle close to 90.0° (*a1* and *b1* variations of 39.1 and 35.6 %, respectively). It is noteworthy that the highest value found for the *a2* and *b2* structures was consistent with the highest stability in aqueous solution. A relationship between the highest μ modulus variation and greater stabilization in solution has already been reported for structures of the series [11].

Conclusions

We concluded that the conformational space of the (4α→6″, 2α→*O*→1″)-phenylflavan substituted with R′=R=OH was described by 48 lowest energy conformers at the calculation level used, the inclusion of solvent by PCM led to the same type of structures as in vacuum, and the stabilization energy in solution was modulated by substitution, increasing in the following order, phenylflavan substituted with R′=R=H<R′=R=OH<(+)-catechin < R′=H, R=OH. All results indicated the importance of Z_2 rotamers in the flavans under study.

The structural parameters of the optimized structures in solution showed small changes from vacuum values. Both in gas phase and in solution, the π bond character decreased on average in the following order, ring D > ring B > ring A > benzene. This decrease was modulated by the substituents, and attenuated in the following order, R′=R=H>R′=H, R=OH>R′=R=OH. Therefore, ring D showed the highest π-electron availability. The intramolecular HB interactions of the catechol rings were characterized using geometric criteria, NBO analysis, and MEP study. For HB interactions in the resorcinol ring, characterization was also drawn from

topological parameters. It was concluded that the solvent changes mainly the CNPs (decrease of electron density in solution), the most affected ones being those accounting for hydroxyl H atoms, and the mean bond ellipticity value for different rings (also a decrease in solution).

We conclude that it was possible to find hyperconjugative interactions that operate in a cooperative way ("delocalization routes"), which allowed us to describe and quantify the interactions between different rings, even when they did not share the same plane. Further MEP analysis allowed us to find the most susceptible sites to electrophilic attack, and also the highest reactivity in aqueous solution. Moreover, the conclusion that the aqueous solvent did not affect all structures of the series uniformly could also be drawn, and changes in the donor role of O─H bonds and oxygen lone pairs were related to changes of MEP.

Molecular polarizability $<\alpha>$ showed low variability when scanning the conformational space. The results indicated the soluble nature of such structures in polar solvents, and that the ability to polarize other atoms or molecules was greater than that reported for the phenylflavan substituted with R′=H, R=OH, and (+)-catechin. The μ modulus value varied over a wide range, but was not useful for distinguishing conformers from each other. The difference between the statistical μ average and the value of the most stable conformer (14.5 %), although highlighting the risk of using the theoretical μ value considering only the most stable conformer, was much lower than that previously found for (+)-catechin (71.4 %). In the series studied, the committed error decreased in the following order, (+)-catechin > phenylflavan substituted with R′=H, R=OH>R′=R=OH, being greater in solution. The values had a non-uniform increase in aqueous solution due to the conformational changes.

We also concluded that the lowest stabilization of the (4α→6″, 2α→*O*→1″)-phenylflavan substituted with R′=R=OH in solution could be related to changes in several electronic properties, among them: electron density at NCPs and mean bond ellipticity (lower decrease), hyperconjugative interactions, MEPs and molecular dipole moment (lower variations).

The accumulated knowledge is relevant in modeling different mechanisms that describe the antioxidant capacity of these compounds, which is currently ongoing in various solvents.

Acknowledgments Thanks are due to National Council of Scientific and Technical Researches of Argentina (CONICET) and Universidad de Buenos Aires (Argentina) for financial support. A.B.P. is a Senior Research Member of CONICET. E.N.B. acknowledges a fellowship of CONICET and Universidad Nacional del Nordeste (Corrientes, Argentina). R.M.L. acknowledges Centro de Cómputos de Alto Desempeño de la Universidad Nacional del Nordeste (CADUNNE) for computational facilities, and financial support of the Secretaria General de Ciencia y Técnica de la Universidad Nacional del Nordeste (Corrientes, Argentina).

References

1. Manach C, Scalbert A, Morand C, Rémésy C, Jiménez L (2004) Polyphenols: food sources and bioavailability. Am J Clin Nutr 79: 727–747
2. Gu L, Kelm M, Hammerstone JF, Beecher G, Holden J, Haytowitz D, Gebhardt S, Prior RL (2003) Concentrations of proanthocyanidins in common foods and estimations of normal consumption. J Nutr 134:613–617
3. Auger C, Al-Awwadi N, Bornet A, Rouanet J-M, Gasc F, Cros G, Teissedre PL (2004) Catechins and procyanidins in Mediterranean diets. Food Res Int 37(3):233–245
4. Yilmaz Y, Toledo RT (2004) Major flavonoids in grape seeds and skins: antioxidant capacity of Catechin, Epicatechin, and gallic acid. J Agric Food Chem 52(2):255–260
5. Hagerman AE, Riedl KM, Jones GA, Sovik KN, Ritchard NT, Hartzfeld PW, Riechel TL (1998) High molecular weight plant polyphenolics (tannins) as biological antioxidants. J Agric Food Chem 46(5):1887–1892
6. Nijveldt RJ, van Nood E, van Hoorn DE, Boelens PG, van Norren K, van Leeuwen PA (2001) Flavonoids: a review of probable mechanism of action and potential applications. Am J Clin Nutr 74(418–425):2001
7. Landrault N, Poucheret P, Ravel P, Gasc F, Cros G, Teissedre PL (2001) Antioxidant capacities and phenolics levels of French wines from different varieties and vintages. J Agric Food Chem 49:3341–3348
8. Heim KE, Tagliaferro AR, Bobilya DJ (2002) Flavonoid antioxidants: chemistry, metabolism and structure-activity relationships. J Nutr Biochem 13(10):572–584
9. Lobayan RM, Jubert AH, Vitale MG, Pomilio AB (2009) Conformational and electronic (AIM/NBO) study of unsubstituted A-type dimeric proanthocyanidin. J Mol Model 15:537–550
10. Lobayan RM, Bentz EN, Jubert AH, Pomilio AB (2010) Theoretical study of Z isomers of A-type dimeric proanthocyanidins substituted with R=H, OH and OCH3: stability and reactivity properties. J Mol Model 16:1895–1909
11. Lobayan RM, Bentz EN, Jubert AH, Pomilio AB (2012) Structural and electronic properties of Z isomers of (4α→6″,2α→O→1″)-phenylflavans substituted with R=H, OH and OCH_3 calculated in aqueous solution with PCM solvation model. J Mol Model 18: 1667–76
12. Bentz EN, Pomilio AB, Lobayan RM (2014) Structure and electronic properties of (+)-catechin: aqueous solvent effects. J Mol Model 20: 2105
13. HyperChem Release 7.5, Hypercube Inc, Gainsville, FL
14. Becke AD (1993) Density-functional thermochemistry. III. The role of exact exchange. J Chem Phys 98:5648–5652
15. Lee C, Yang W, Parr RG (1988) Development of the Colle- Salvetti correlation energy formula into a functional of the electron density. Phys Rev B 37:785–789
16. Frisch MJ, Trucks GW, Schlegel HB, Scuseria GE, Robb MA, Cheeseman JR, Montgomery JA, Vreven T Jr, Kudin KN, Burant JC, Millam JM, Iyengar SS, Tomasi J, Barone V, Mennucci B, Cossi M, Scalmani G, Rega N, Petersson GA, Nakatsuji H, Hada M, Ehara M, Toyota K, Fukuda R, Hasegawa J, Ishida M, Nakajima T, Honda Y, Kitao O, Nakai H, Klene M, Li X, Knox JE, Hratchian HP, Cross JB, Adamo C, Jaramillo J, Gomperts R, Stratmann RE, Yazyev O, Austin AJ, Cammi R, Pomelli C, Ochterski JW, Ayala PY, Morokuma K, Voth GA, Salvador P, Dannenberg JJ, Zakrzewski VG, Dapprich S, Daniels AD, Strain MC, Farkas O, Malick DK, Rabuck AD, Raghavachari K, Foresman JB, Ortiz JV, Cui Q, Baboul AG, Clifford S, Cioslowski J, Stefanov BB, Liu G, Liashenko A, Piskorz P, Komaromi I, Martin RL, Fox DJ, Keith T, Al-Laham MA, Peng CY, Nanayakkara A, Challacombe M, Gill

PMW, Johnson B, Chen W, Wong MW, Gonzalez C, Pople JA (2003) Gaussian 03, revision B.02. Gaussian Inc, Pittsburgh
17. Miertuš S, Scrocco E, Tomassi J (1981) Electrostatic interaction of a solute with a continuum. A direct utilization of ab initio molecular potentials for the prevision of solvent effects. Chem Phys 55:117–129
18. Flúkiger P, Lúthi HP, Portmann S, Weber J (2000) MOLEKEL 4.0. Swiss Center for Scientific Computing, Manno, Switzerland
19. Lu T, Chen F (2012) Multiwfn: A multifunctional wavefunction analyzer. J Comput Chem 33:580–592
20. Biegler-Koning FW, Bader RFW, Tang TH (1982) Calculation of the average properties of atoms in molecules.II. J Comput Chem 3: 317–328
21. Glendening ED, Reed AE, Carpenter JE, Weinhold F NBO 3.1. Program as implemented in the Gaussian 03 package
22. Estévez L, Mosquera R (2007) A density functional theory study on pelargonidin. J Phys Chem A 111:11100–9
23. Glossman-Mitnik D, Mendoza-Wilson AM, Lardizabal-Gutiérrez D, Torres-Moye E, Fuentes-Cobas L, Balandrán-Quintana R, Camacho-Dávila A, Quintero-Ramos A (2007) Optimized structure and thermochemical properties of flavonoids determined by the CHIH(medium) DFT model chemistry versus experimental techniques. J Mol Struct 871:114–130
24. Zhang HY, Sun YM, Wang XL (2003) Why B-ring is the active center for genistein to scavenge peroxyl radical: A DFT study. Bioorg Med Chem Lett 13:909–911
25. Aparicio S (2010) A systematic computational study on flavonoids. Int J Mol Sci 11:2017–38
26. Desiraju GR, Steiner T (1999) The weak hydrogen bond in structural chemistry and biology. Oxford University Press, New York
27. Popelier PLA (1998) Characterization of a dihydrogen bond on the basis of the electron density. J Phys Chem A 102:1873–1878
28. Koch U, Popelier P (1995) Characterization of C-H-O hidrogen bonds on the basis of the charge density. J Phys Chem 99:9747–9754
29. Carroll MT (1988) Bader RFW (1988) An analysis of the hydrogen bond in BASE-HF complexes using the theory of atoms in molecules. Mol Phys 65:695–722
30. Politzer P, Truhlar DG (1981) Chemical applications of atomic and molecular electrostatic potentials. Plenum, New York
31. Bentz EN, Pomilio AB (2014) Lobayan RM (2014) Exploratory conformational study of (+)- catechin. Modeling of the polarizability and electric dipole moment. J Mol Model 20:2522
32. Nguyen TV, Pratt DW (2006) Permanent electric dipole moments of four tryptamine conformers in the gas phase: a new diagnostic of structure and dynamics. J Chem Phys 124:1216–1219
33. Antonczak S (2008) Electronic description of four flavonoids revisited by DFT method. J Mol Struct THEOCHEM 856:38–45